



HAL
open science

Magneto-mechanical analysis of magnetic gear pole pieces ring from analytical models for wind turbine applications

Melaine Desvaux, Bernard Multon, Hamid Ben Hamed, Stéphane Sire

► To cite this version:

Melaine Desvaux, Bernard Multon, Hamid Ben Hamed, Stéphane Sire. Magneto-mechanical analysis of magnetic gear pole pieces ring from analytical models for wind turbine applications. *Wind Engineering*, 2018, 42 (4), pp.276-285. 10.1177/0309524X18777314 . hal-01853746

HAL Id: hal-01853746

<https://hal.science/hal-01853746>

Submitted on 11 Jul 2023

HAL is a multi-disciplinary open access archive for the deposit and dissemination of scientific research documents, whether they are published or not. The documents may come from teaching and research institutions in France or abroad, or from public or private research centers.

L'archive ouverte pluridisciplinaire **HAL**, est destinée au dépôt et à la diffusion de documents scientifiques de niveau recherche, publiés ou non, émanant des établissements d'enseignement et de recherche français ou étrangers, des laboratoires publics ou privés.

Magneto-mechanical analysis of magnetic gear pole pieces ring from analytical models for wind turbine applications

M Desvaux¹, B Multon¹, H Ben Ahmed¹ and S Sire²

Abstract

This article deals with the structural behavior of a multi-bar system which maintains pole pieces in a concentric magnetic gear. Simplified analytic magnetic and mechanical models of the system are proposed in order to be integrated in a multi-criteria global optimization for the sizing of a magnetic gear in wind power applications. For this purpose, the reduction of the computation time is taken into account. The geometry of the support bar subsystem is defined and a Q bar structure is proposed. The magnetic study is based on Maxwell's equations and subdomain method in order to determine variable radial and tangential magnetic loads. The mechanical study is based on a multibody model with different bars stiffnesses which are determined from a one-dimensional model. Variable radial and tangential magneto-mechanical pole pieces loads (magnetic load and weight) are also considered. An example of a magnetic gear with 172 pole pieces (i.e. 6-MW wind turbine) is proposed to analyze the mechanical behavior and also the computation time.

Keywords

Analytical model, computation time, laminated pole pieces, magnetic gear, magnetic load, mechanical sizing, multibody model, support bar

Introduction

The development of electricity production from renewable energy is currently expanding rapidly (IRENA, 2017). This development includes the conversion of wind energy resources from either onshore or offshore localization (Hau, 2013; Lacal Arántegui and Serrano Gonzáles, 2015; Larsen et al., 2005; Larsen and Sønnderberg Petersen, 2014). To perform an energy conversion from wind, different conversion chains are proposed from different wind turbine manufacturers (Larsen and Sønnderberg Petersen, 2014). On one side, there are the indirect drive designs with multi-stages of mechanical gears like the wind turbine SL-6000, a 6.0-MW wind turbine with three-stage mechanical gears, or the wind turbine V164, a 8.0-MW wind turbine with a single-stage mechanical gear (Larsen and Sønnderberg Petersen, 2014). On the other side, there are the direct drive designs without mechanical gearbox like the wind turbine Haliade (6 MW) or E126 (7.5 MW) (Larsen and Sønnderberg Petersen, 2014).

It has been shown that indirect drive designs provide a lower capital expenditure and lower masses than the direct drive designs and this becomes more critical when the power of the wind turbine increases, as for offshore wind turbines (Henriksen and Jensen, 2012; Polinder et al., 2006). In return, mechanical gearboxes induce production interruptions and repairs, which increase operating costs (Keller et al., 2016; Teng et al., 2016; Thor, 2008). Aiming to reduce the overall life cycle cost, a potential solution is to combine a generator with a magnetic gear in order to obtain a fully magnetic indirect drive designs (Desvaux et al., 2016; Matt et al., 2012). For these designs, an attractive topology of magnetic gear has been proposed by Martin (1968) and used in different studies (Atallah et al., 2008; Atallah and Howe, 2001; Rasmussen et al., 2005; Wang et al., 2009).

¹SATIE Laboratory, ENS Rennes, Université Bretagne Loire, CNRS, Bruz, France

²IRDL—FRE CNRS 3744, Université de Bretagne Occidentale, Brest, France

Corresponding author:

M Desvaux, SATIE Laboratory, ENS Rennes, Université Bretagne Loire, CNRS, 35044 Bruz, France.

Email: melaine.desvaux@ens-rennes.fr

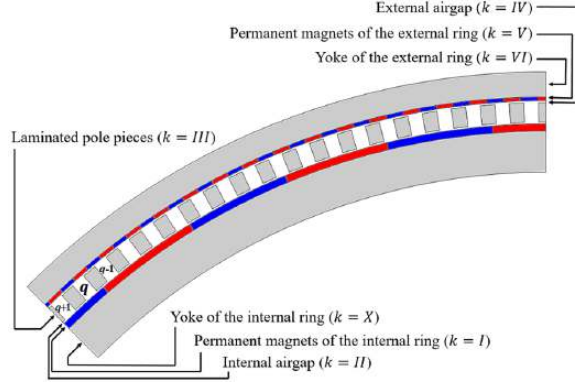


Figure 1. Part of the magnetic region of a magnetic gear.

This concentric magnetic gear architecture shown in Figure 1 potentially offers a higher performance with a high torque density and a high reliability than mechanical gearboxes (Gouda et al., 2011) and even more for high-torque applications like offshore wind turbine (of the order of a few MN m and a few MW) with only magnetic part consideration (Matt et al., 2012). However, no magneto-mechanical sizing has been done on this magnetic gear (with an approach similar than (Zavvos et al., 2011) for a wind turbine generator) and it seems to have weaknesses in terms of mechanical strength since some parts are subjected to variable radial and tangential loads from the magnetic field. Indeed, ferromagnetic pole pieces are very elongated structures laminated perpendicular to the axis of rotation (to minimize iron losses and conserve a high efficiency of the system) and subjected to a variable magnetic load.

The weakness of this part of the system raises the question of the possibility to maintain mechanically the laminated pole pieces without lessening the magnetic properties (therefore, without increasing air gaps and modifying magnetic field) in high-power wind turbine applications (i.e. high dimensions and high pole numbers of the magnetic gear). It is then necessary to evaluate the stiffness of the pole piece structure for different configurations. This evaluation must be done in a global multi-criteria mechatronic optimization.

The major contribution of this work is the definition of analytical models (based on subdomain method in magnetism and multibody model in mechanics) of the pole pieces ring in order to evaluate quickly different mechanical criteria based on displacement and stress distributions and evolutions. These analytical models do not consider the coupling between magnetic loads and displacement (due to the low value of displacement) and could be integrated in a multi-criteria mechatronic optimization of a magnetic gear for wind turbine applications.

Design of the pole pieces ring

As shown in Figure 1, the magnetic gear is composed of three rings: a ring with p_{LPN} low pole number of pole pairs of permanent magnets and a ferromagnetic yoke, a ring with p_{HPN} high pole number of pole pairs of permanent magnets and a ferromagnetic yoke, a ring with Q ferromagnetic pole pieces (an example is given in Figure 1 with $p_{LPN} = 20$, $p_{HPN} = 131$, and $Q = 151$). To achieve the power transmission, three rings' pole numbers must respect equation (1) (Atallah et al., 2004). When the pole pieces ring is fixed, the gear ratio G_m is given by equation (2) (Atallah et al., 2004)

$$p_{HPN} + p_{LPN} = Q \quad (1)$$

$$G_m = -\frac{p_{HPN}}{p_{LPN}} \quad (2)$$

The rotation of the two permanent magnet rings generates two rotating magneto-motive forces. Pole pieces are then subjected to a rotating flux density which imposes to laminate the pole pieces in order to reduce iron losses (Desvaux et al., 2017b; Rasmussen et al., 2011). The rotating flux also generates variable radial and tangential loads on different pole pieces (Filippini and Alotto, 2017). Pole pieces must then be supported by a multi-bar system which must resist to the transmitted magneto-mechanical loads. For high-power applications like offshore wind turbine, the number of pole increases with the diameter. A consequence can be a decrease in the structure rigidity.

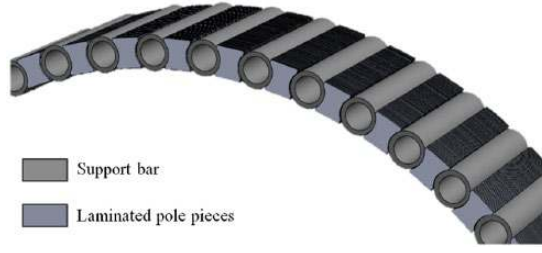


Figure 2. Pole pieces ring with support bars (end bells are not represented).

To support the laminated pole pieces of the magnetic gear, the support bar geometry shown in Figure 2 is proposed. The support bars are composed of a massive magnetic insulator steel and a magnetic and electrical insulator skin. These support bars do not lessen the magnetic density of the system since they do not need to increase the airgap dimensions, but the geometry adaptation of the pole pieces slightly modify the magnetic field. Support bar will then transmit the magneto-mechanical load of the laminated pole pieces to the structural parts. Support bars are thus subjected to variable radial and tangential magnetic load; their induced displacements and stresses must be then taken into account for their sizing (see Desvaux et al., 2016).

Magnetic analytical model

To compute a two-dimensional (2D) magnetic load analytically, an adapted geometry of the pole pieces is considered (see Figure 3(a)) since the geometry presented in Figure 2 (which takes into account support bars) might make the model complicated and therefore greatly increase the computation time (see Figure 3(b)). For the geometry of magnetic gear without support bars, we need first to determine the magnetic field repartition with the radial flux density $B_r^{(k)}$ and tangential flux density $B_t^{(k)}$ as defined in Lubin et al. (2010) and Desvaux et al. (2017d) for the k region of the magnetic gear (according to Figure 1). It is then possible to compute the Maxwell stress tensor $\overset{=}{\sigma}^{(k)}$ as defined in equation (3) for the k region of the magnetic gear. To compute the radial and tangential load of the pole piece q from the Maxwell tensor, in accordance with Figure 3(a), the magnetic radial load $F_r^{(q)}$ is given by equation (4) and the magnetic tangential load $F_t^{(q)}$ is given by equation (5) for the pole piece q with the hypothesis of small opening angle of pole pieces (Filippini and Alotto, 2017)

$$\overset{=}{\sigma}^{(k)}(r, \alpha) = \begin{pmatrix} \sigma_{rr}^{(k)} & \sigma_{r\alpha}^{(k)} & 0 \\ \sigma_{r\alpha}^{(k)} & \sigma_{\alpha\alpha}^{(k)} & 0 \\ 0 & 0 & 0 \end{pmatrix} = \frac{1}{\mu_0} \begin{pmatrix} B_r^{(k)2} / 2 - B_\alpha^{(k)2} / 2 & B_r^{(k)} \cdot B_\alpha^{(k)} & 0 \\ B_r^{(k)} \cdot B_\alpha^{(k)} & B_\alpha^{(k)2} / 2 - B_r^{(k)2} / 2 & 0 \\ 0 & 0 & 0 \end{pmatrix} \quad (3)$$

$$\begin{aligned} F_r^{(q)} &= \bar{e}_r \cdot \iint \overset{=}{\sigma}^{(k,q)} \cdot \bar{e}_r \cdot dS \\ &= \bar{e}_r \cdot \int_{z=0}^L \int_{\alpha_q+\beta}^{\alpha_{q+1}} \overset{=}{\sigma}^{(IV)}(R_M^{(III)}, \alpha) \cdot \bar{e}_r \cdot R_M^{(III)} \cdot d\alpha \cdot dz \\ &\quad - \bar{e}_r \cdot \int_{z=0}^L \int_{\alpha_q+\beta}^{\alpha_{q+1}} \overset{=}{\sigma}^{(II)}(R_m^{(III)}, \alpha) \cdot \bar{e}_r \cdot R_m^{(III)} \cdot d\alpha \cdot dz \\ &\quad + \bar{e}_\alpha \cdot \int_{z=0}^L \int_{R_n^{(III)}}^{R_M^{(III)}} \overset{=}{\sigma}^{(III,q)}(r, \alpha_q + \beta) \cdot \bar{e}_r \cdot dr \cdot dz \\ &\quad - \bar{e}_\alpha \cdot \int_{z=0}^L \int_{R_n^{(III)}}^{R_M^{(III)}} \overset{=}{\sigma}^{(III,q+1)}(r, \alpha_{q+1}) \cdot \bar{e}_r \cdot dr \cdot dz \end{aligned} \quad (4)$$

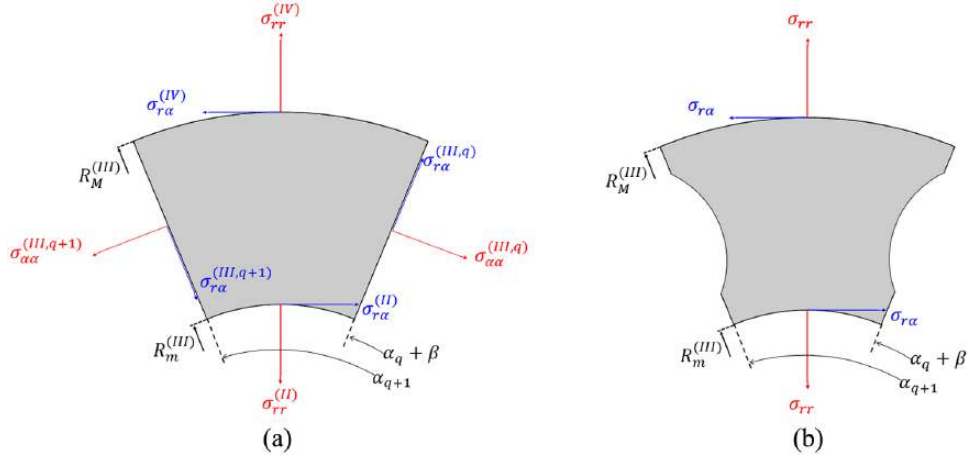


Figure 3. (a) Parametrization of the adapted pole piece for radial and tangential loads computation and (b) pole piece geometry considering support bars.

$$\begin{aligned}
 F_t^{(q)} &= \overline{e}_n \cdot \iint \overline{\sigma}^{(k,q)} \cdot \overline{e}_\alpha \cdot dS \\
 &= \overline{e}_r \cdot \int_{z=0}^L \int_{\alpha_q + \beta}^{\alpha_{q+1}} \overline{\sigma}^{(IV)}(R_M^{(III)}, \alpha) \cdot \overline{e}_\alpha \cdot R_M^{(III)} \cdot d\alpha \cdot dz \\
 &\quad - \overline{e}_r \cdot \int_{z=0}^L \int_{\alpha_q + \beta}^{\alpha_{q+1}} \overline{\sigma}^{(II)}(R_m^{(III)}, \alpha) \cdot \overline{e}_\alpha \cdot R_m^{(III)} \cdot d\alpha \cdot dz \\
 &\quad + \overline{e}_\alpha \cdot \int_{z=0}^L \int_{r=R_m^{(III)}}^{R_M^{(III)}} \overline{\sigma}^{(III,q)}(r, \alpha_q + \beta) \cdot \overline{e}_\alpha \cdot dr \cdot dz \\
 &\quad + \overline{e}_\alpha \cdot \int_{z=0}^L \int_{r=R_m^{(III)}}^{R_M^{(III)}} \overline{\sigma}^{(III,q+1)}(r, \alpha_{q+1}) \cdot \overline{e}_\alpha \cdot dr \cdot dz
 \end{aligned} \tag{5}$$

To compute magnetic loads by considering the support bar geometry proposed in Figure 2, it is possible to use 2D magnetic finite element model (FEM). Figure 4 shows first that the magnetic loads obtained from a 2D FEM with the adapted geometry of pole pieces are in agreement with magnetic loads obtained considering the support bars (see Figure 2) for the magnetic gear (Desvaux et al., 2017c). Figure 4 also shows that the magnetic load obtained analytically (seen in Filippini and Alotto, 2017) are close enough to those obtained with 2D FEM with the same geometry. These two results validate the consideration of the adapted geometry necessary to determine magnetic load analytically. Moreover, the analytical model permits to divide the computation time by 1000 (15,000 s vs 15 s, with the same discretization of rotation (30 positions)) and it offers a computation time adapted for a global mechatronic optimization.

Mechanical model

Multibody model

Loads that generate stresses and displacements are the magnetic radial and tangential load ($\overline{F_r^{(q)}}$ and $\overline{F_\alpha^{(q)}}$) and the weight of the structure for the Q pole pieces and Q support bars (q corresponds to the number of the pole pieces, $1 \leq q \leq Q$). For the magnetic gear (Desvaux et al., 2017c), the weight reaches approximately 60N for a support bar and 120N for a pole piece. The weight will then have a small impact on the mechanical behavior in comparison to the magnetic load for this magnetic gear (see Figure 4). The geometry of the structural part of the pole pieces ring includes support bars and end bells. It is possible to consider that a support bar is equivalent to a fixed-end beam and that the end bells have a negligible

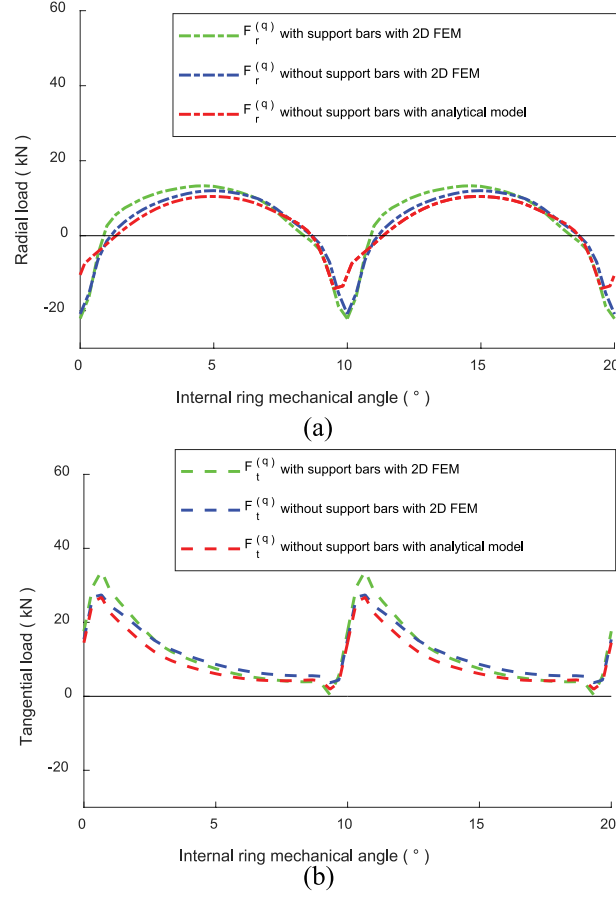


Figure 4. Comparison between the magnetic loads obtained from the 2D finite element model with the support bar geometry and from the analytical model without considering support bar geometry for the magnetic gear: (a) radial load and (b) tangential load for the magnetic gear (Desvaux et al., 2017c).

deformation compared to support bars. Considering that the magnetic load and the weights are applied in the middle of the pole pieces, the pole pieces ring parametrization and modeling is described in Figure 5(a) and the multibody model described in Figure 5(b) is proposed (Desvaux et al., 2017a).

As shown in Figure 5(b), the multibody model is composed of $4Q$ bodies $S_i^{(q)}$ (with $i = 1, \dots, 4$) and $4Q$ degrees of freedom ($2Q$ translation and $2Q$ rotation) (Desvaux et al., 2017a). The $2Q$ translations are linked to the stiffness of the support bars and the $2Q$ rotations correspond to the contacts between pole pieces and support bars. The stiffness of the support bars is determined from a fixed-end beam one-dimensional (1D) model. The stiffness of pole pieces is considered negligible in this study because they are laminated.

This multibody model includes $8Q$ unknowns. They correspond to the $2Q$ stiffnesses defined in equation (6), the $2Q$ fixed-end reactions at the end of the support bars $(\overline{X_1^{(q)}}, \overline{Y_2^{(q)}})$ and the $4Q$ reactions from the contact between pole pieces and support bars as shown in Figure 5(b) $(\overline{X_3^{(q)}}, \overline{Y_3^{(q)}}, \overline{X_4^{(q)}}, \overline{Y_4^{(q)}})$

$$\begin{cases} \overline{T_x^{(q)}} = k_x^{(q)} \cdot x^{(q)} \cdot \overline{x_{S,q}} \\ \overline{T_y^{(q)}} = k_y^{(q)} \cdot y^{(q)} \cdot \overline{y_{S,q}} \end{cases} \quad (6)$$

Displacement evaluation

From equilibriums proposed in Desvaux et al. (2017a), the displacements of the support bars generated by the magnetic load and weight can be determined and the reactions at the end of the support bars too. It is then possible to show the

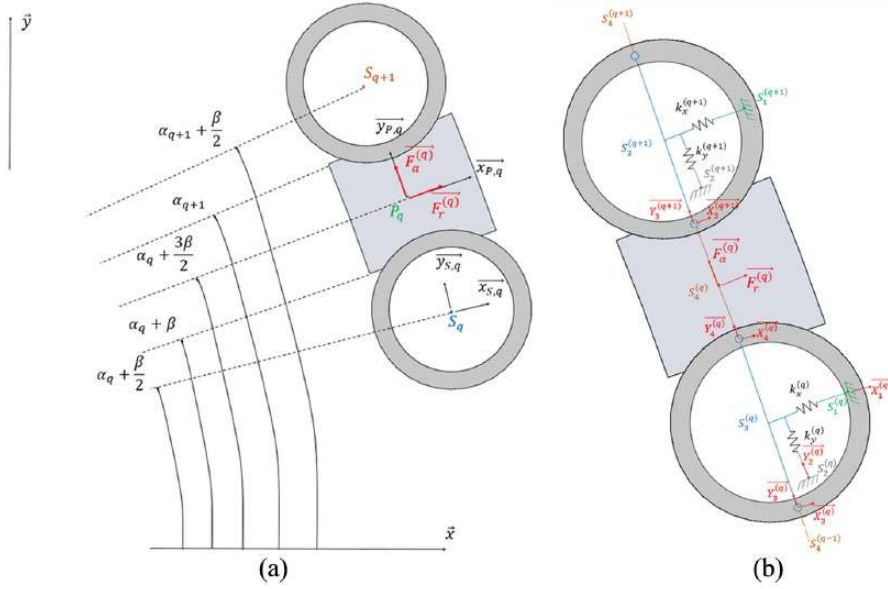


Figure 5. (a) Parametrization and modeling of the pole pieces ring; and (b) multibody modeling of the pole pieces ring with the definition of the different loads and bodies.

radial and tangential displacements of different support bars as shown in Figure 6 for a support bar placed horizontally (the weight correspond to a tangential load), for a support bar placed vertically (the weight correspond to a radial load), and for a support bar placed arbitrary, for the magnetic gear (Desvaux et al., 2017c).

Figure 6 shows that support bars are approximately subjected to the same displacement since the weight is negligible compared to the magnetic load. Then, the evolution of the displacements has the same form than the evolution of the magnetic load (Figure 4). Moreover, the periodicity T of the displacements corresponds to the periodicity of the magnetic load which depends on the rotational speed and the pole pair configuration of the rings as shown in equation (7) with $\Omega_{LPN/0}$ —the rotation speed of the high-speed rotor and $\Omega_{HPN/0}$ —the rotation speed of the low-speed rotor

$$T = \frac{2\pi}{P_{LPN} \cdot \Omega_{LPN/0}} = \frac{2\pi}{P_{HPN} \cdot \Omega_{HPN/0}} \quad (7)$$

In order to size the pole pieces ring, we propose like Desvaux et al. (2016) and Zavvos et al. (2011) to impose that the radial displacement of support bars $x^{(q)}$ must be lower than 10% of the airgap δ (0.5 mm for the magnetic gear; Desvaux et al., 2017c) and the relative twist generated by the tangential displacement $y^{(q)}$ must be lower than 0.01° (equation (8))

$$\left\{ \begin{array}{l} x^{(q)} < \delta * 10\% \\ \tan \left(\frac{y^{(q)}}{\frac{R_m^{(III)} + R_M^{(III)}}{2}} \right) < 0.01^\circ \end{array} \right. \quad (8)$$

Stress evaluation

In order to evaluate if the stress in the support bars does not exceed a critical value, it is necessary to analyze where the maximal stress values are. For a cylindrical fixed-end beam with a point load in the center of the beam, the maximal stress is obtained at the ends of the beam (equation (9)) with parameters defined in Figure 7. At the end of each cylindrical support bar, the maximal stress is located on the external radius of the cross section. Moreover, considering the dimensions of the support bars, on the external radius of the support bars, $\sigma_{xz}^{(q)} \ll \sigma_{zz}^{(q)}$ and $\sigma_{yz}^{(q)} \ll \sigma_{zz}^{(q)}$. The von Mises stress $\sigma_{VM}^{(q)}$

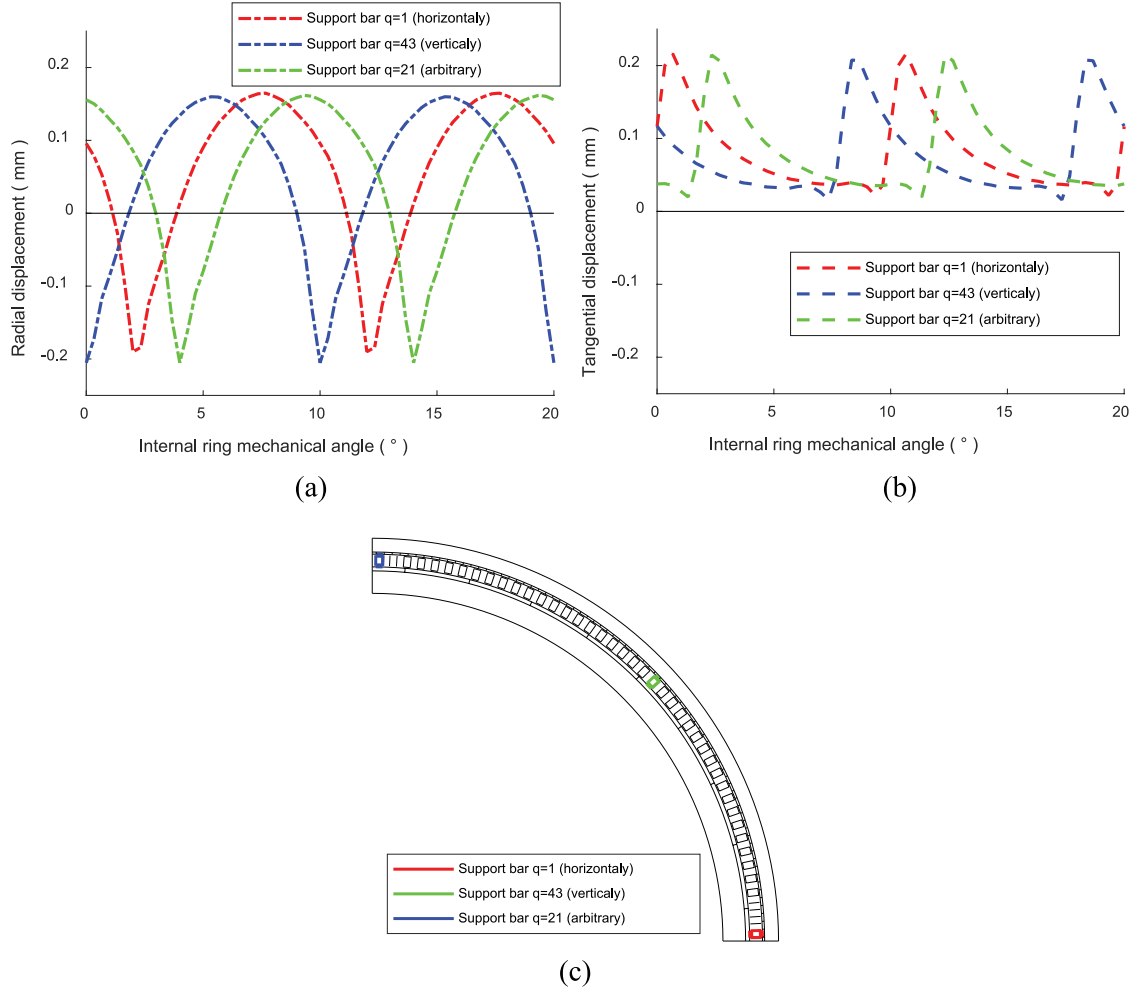


Figure 6. Evolution of (a) the radial displacement and (b) tangential displacement of support bars due to the magnetic loads and the weight for the magnetic gear (Desvaux et al., 2017c) with a constant rotational speed of 13 r/min for the external ring and 85 r/min for the internal ring with (c) the position of the three studied support bars.

is then directly equal to the normal stress $\sigma_{zz}^{(q)}$. In order to evaluate the maximal stress value at a position of the magnetic gear, the critical value $\sigma_{VM\ max}^{(q)}$ is obtained in the same direction than the load $\overline{T}^{(q)} = \overline{T}_x^{(q)} + \overline{T}_y^{(q)}$ and must be lower than the yield stress of the material σ_y (equation (9))

$$\left\{ \begin{array}{l} \sigma_{zz}^{(q)}(x, y, 0) = \frac{T_x^{(q)} \cdot L}{8 \cdot I_{Gy}} x - \frac{T_y^{(q)} \cdot L}{8 \cdot I_{Gx}} y \\ \sigma_{VM\ max}^{(q)} = \frac{T^{(q)} \cdot L \cdot R}{8 \cdot I_{Gy}} < \sigma_y \\ T^{(q)} = \sqrt{T_x^{(q)2} + T_y^{(q)2}} \end{array} \right. \quad (9)$$

Due to the rotation of the magnetic field, the maximum stress is located on the external radius at the end of the beam, and this location changes with the mechanical angle, as shown in Figure 8 for the magnetic gear (Desvaux et al., 2017c) with $\theta^{(q)}$ the orientation $\overline{T}^{(q)}$ of defined in Figure 7 and $\sigma_{VM\ max}^{(q)}$ in equation (9). It is then necessary to evaluate the

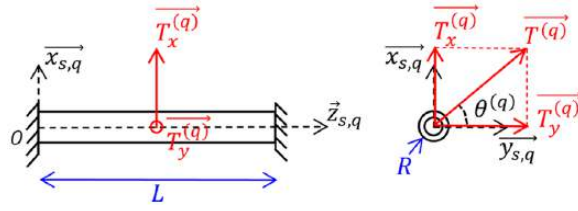


Figure 7. Parametrization of the support bar fixed-end beam modelization.

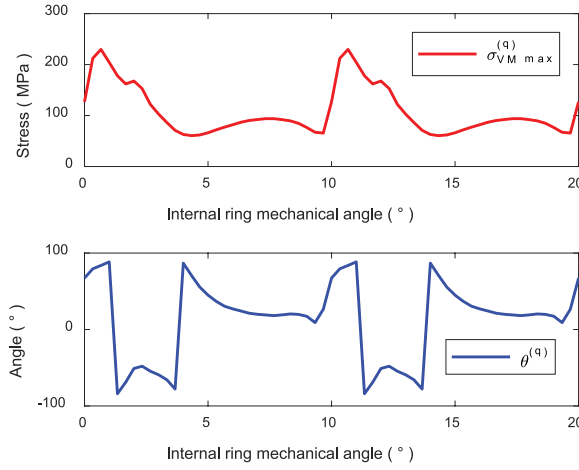


Figure 8. Evolution of the maximal stress value $\sigma_{VM\max}^{(q)}$ generated by the magnetic load $\vec{T}^{(q)}$ with the orientation $\theta^{(q)}$ for the magnetic gear (Desvaux et al., 2017c). $\theta^{(q)}$ also corresponds to the position of the maximal stress value $\sigma_{VM\max}^{(q)}$ on the external radius at the end of the beam.

maximal stress value for different positions (see Figure 8) and evaluate the evolution of the stress at different points on the external radius at the end of the beam as shown in Figure 9 for the magnetic gear (Desvaux et al., 2017c). The different stress evolutions proposed in Figure 9 show a cyclic loading with a mean stress different from zero, which suggests the use of a fatigue criterion for sizing the support bars (equation (10)) considering a given N number of cycles

$$\Delta\sigma_{zz} < \Delta\sigma_{limit} \quad (10)$$

Since the magnetic loads are determined, the evaluation of stresses and displacements with the multibody analytical model is very quick. Indeed, with a discretization of the rotation in 30 positions, the computation time is equal to 1.5 s. This analytical model permits to reduce strongly the computation time compared to three-dimensional (3D) FEM since with the same hypothesis, the computation is done in 5000 s. From the magnetic and mechanical models, it is then possible to evaluate for the radial displacement, the relative twist generated by tangential displacement, the maximal value of the von Mises stress, and the normal stress amplitude needed for a fatigue assessment with a computation time lower than 20 s, which is adapted to a multi-criteria optimization procedure.

Conclusion

This article proposes magnetic and mechanical analytical models and an analysis of the mechanical behavior of the pole pieces ring in a magnetic gear. The analysis permits to show that four mechanical criteria must be evaluated to size correctly the pole pieces ring of the magnetic gear:

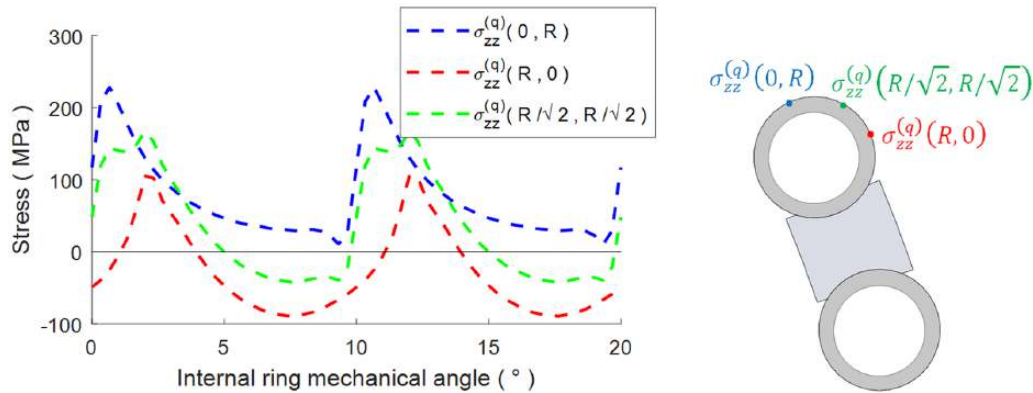


Figure 9. Stress evolution on the external radius of a support bar of the magnetic gear (Desvaux et al., 2017c).

- The radial displacement of support bars (equation (8)).
- The relative twist generated by tangential displacement (equation (8)).
- The maximal von Mises stress value (equation (9)).
- The stress amplitude for a fatigue assessment (equation (10)).

Moreover, the analytical models developed in this article permit to strongly reduce the computation time since the evaluation is done in approximately 20s with the analytical models versus 20,000s with mechanical 3D FEM and magnetic 2D FEM. Models proposed in this article are then adapted to a multi-criteria optimization procedure that we need to perform in prospect. This procedure also contains mechanical analytical models of the different other structural parts of the magnetic gear. However, it is possible to analyze the dynamic aspects generated by the magnetic cyclic load.

Declaration of conflicting interests

The author(s) declared no potential conflicts of interest with respect to the research, authorship, and/or publication of this article.

Funding

The authors thank the French Ministry of Research for the funding of the Doctoral Thesis Grant and the company Jeumont Electric for its partnership and financial contribution to this work.

References

- Atallah K and Howe D (2001) A novel high-performance magnetic gear. *IEEE Transactions on Magnetics* 37(4): 2844–2846.
- Atallah K, Calverley SD and Howe D (2004) Design, analysis and realisation of a high-performance magnetic gear. *IEE Proceedings—Electric Power Applications* 2004; 151(2): 135–143.
- Atallah K, Rens J, Mezani S, et al. (2008) A novel “pseudo” direct-drive brushless permanent magnet machine. *IEEE Transactions on Magnetics* 44(11): 4349–4352.
- Desvaux M, Le Goff Latimier R, Multon B, et al. (2016) Design and optimization of magnetic gears with arrangement and mechanical constraints for wind turbine applications. In: *Eleventh international conference on ecological vehicles and renewable energies (EVER)*, Monte Carlo, 6–8 April.
- Desvaux M, Multon B, Ben Ahmed H, et al. (2017a) Supporting the laminated ferromagnetic pole pieces in a magnetic gear: A structure behaviour analysis from a multibody model. In: Carvalho JCM, Martins D, Simoni R, et al. (eds) *International symposium on multibody systems and mechatronics—MuSMe 2017: Multibody mechatronic systems*, vol. 54. Florianopolis, Brazil: Springer, 2017, pp. 85–94.
- Desvaux M, Multon B, Sire S, et al. (2017b) Analytical iron loss model for the optimization of magnetic gear. In: *IEEE international electric machines and drives conference (IEMDC)*, Miami, FL, 21–24 May.
- Desvaux M, Multon B, Sire S, et al. (2017c) Optimisation bi-objectif explicite d’un multiplicateur magnétique pour l’éolien. In: *Conférence nationale des Jeunes Chercheurs en Génie Electrique (JCGE 2017)*. Available at: https://jcge2017.sciencesconf.org/data/pages/Programme_web_1.pdf
- Desvaux M, Traullé B, Le Goff Latimier R, et al. (2017d) Computation time analysis of the magnetic gear analytical model. *IEEE Transactions on Magnetics* 53(5): 1–10.

- Filippini M and Alotto P (2017) Coaxial magnetic gears design and optimization. *IEEE Transactions on Industrial Electronics* 46: 9934–9942.
- Gouda E, Mezani S, Baghli L, et al. (2011) Comparative study between mechanical and magnetic planetary gears. *IEEE Transactions on Magnetics* 47(2): 439–450.
- Hau E (2013) The wind resource. In: Hau E (ed.) *Wind Turbines*, Springer, 2013, pp. 505–547.
- Henriksen ML and Jensen BB (2012) Comparison of Megawatt-class permanent magnet wind turbine generator concepts. In: *Proceedings of EWEA*, Copenhagen, Denmark, 16–19 April.
- IRENA (2017) *REthinking energy 2017*, vol. 55, July. Available at: https://www.irena.org/DocumentDownloads/Publications/IRENA_REthinking_Energy_2017.pdf
- Keller J, Guo Y and Sethuraman L (2016) *Gearbox reliability collaborative investigation of gearbox motion and high-speed-shaft loads*. Technical report NREL/TP-5000-65321. Available at: <https://www.nrel.gov/docs/fy16osti/65321.pdf>
- Lacal Arántegui R and Serrano González J (2015) Wind status report: Technology, market and economic aspects of wind energy in Europe. JRC. Available at: http://publications.jrc.ec.europa.eu/repository/bitstream/JRC85756/ldna26266enn_2013_jrc_wind_status_report_final.pdf
- Larsen H and Sønderberg Petersen L (2014) DTU International Energy Report 2014: *Wind energy—drivers and barriers for higher shares of wind in the global power generation mix*. Copenhagen, Denmark.
- Larsen JHM, Soerensen HC, Christiansen E, et al. (2005) Experiences from Middelgrunden 40 MW offshore wind farm. In: *Copenhagen offshore wind*, Copenhagen, Denmark, 26–28 October.
- Lubin T, Mezani S and Rezzoug A (2010) Analytical computation of the magnetic field distribution in a magnetic gear. *IEEE Transactions on Magnetics* 46(7): 2611–2621.
- Martin TB (1968) Magnetic transmission. Patent US3378710.
- Matt D, Julien J and Ziegler N (2012) Design of a mean power wind conversion chain with a magnetic speed multiplier. *Advances in Wind Power*. InTech.
- Polinder H, Van Der Pijl FF, De Vilder GJ, et al. (2006) Comparison of direct-drive and geared generator concepts for wind turbines. *IEEE Transactions on Energy Conversion* 21(3): 725–733.
- Rasmussen PO, Andersen TO, Jørgensen FT, et al. (2005) Development of a high-performance magnetic gear. *IEEE Transactions on Industry Applications* 41(3): 764–770.
- Rasmussen PO, Frandsen TV, Jensen KK, et al. (2011) Experimental evaluation of a motor integrated permanent magnet gear. In: *IEEE energy conversion congress and exposition (ECCE)*, Phoenix, AZ, 17–22 September, pp. 3982–3989. New York: IEEE.
- Teng W, Ding X, Zhang X, et al. (2016) Multi-fault detection and failure analysis of wind turbine gearbox using complex wavelet transform. *Renewable Energy* 93: 591–598.
- Thor SE (2008) Wind turbine drivetrain dynamics and reliability. In: *57th IEA topical expert meeting*, Jyväskylä, Finland, 4–5 September.
- Wang L, Shen JX, Luk PCK, et al. (2009) Development of a magnetic-geared permanent-magnet brushless motor. *IEEE Transactions on Magnetics* 45(10): 4578–4581.
- Zavvos A, McDonald AS and Mueller M (2011) Structural optimisation tools for iron cored permanent magnet generators for large direct drive wind turbines. In: *IET conference on renewable power generation (RPG 2011)*, Edinburgh, 6–8 September.